Influence of tool geometry and rotational speed on mechanical properties and defect formation in friction stir lap welded 5456 aluminum alloy sheets

Emad Salari[a], Mohammad Jahazi[b,1], Alireza Khodabandeh[a], Hadi Ghasemi-Nanesa[b]

[a]*Science and Research Branch, IAU, 1477893855 Tehran, Iran*

[b] *Department of Mechanical Engineering, École de Technologie Supérieure, 1100 rue Notre-Dame Ouest, Montréal (QC) H3C1K3 Canada.*

Abstract

Friction stir welding of AA5456 aluminum alloy in lap joint configuration is with two different tempers, T321 and O, and different thicknesses, 5mm and 2.5mm was investigated. The influences of tool geometry and various rotational speeds on macrostructure, microstructure and joint strength are presented. Specifically, four different tool pin profiles (a conical thread pin, a cylindrical–conical thread pin, a stepped conical thread pin and Flared Triflute pin tool) and two rotational speeds, 600 and 800 rpm, were used. The results indicated that, tool geometry influences significantly material flow in the nugget zone and accordingly control the weld mechanical properties. Of particular interest is the stepped conical threaded pin, which is introduced for the first time in the present investigation. Scanning electron microscopy investigation of the fracture location of samples was carried out and the findings correlated with tool geometry features and their influences on material flow and tension test results. The optimum microstructure and mechanical properties were obtained for the joints produced with the stepped conical thread pin profile and rotational speed of 600 rpm. The characteristics of the nugget zone microstructure, hooking height, and fracture location of the weld joints were used as criteria to quantify the influence of processing conditions on joint performance and integrity. The results are interpreted in the framework of physical metallurgy properties and compared with published literature.

Keywords: Friction stir welding; Lap joint, Aluminum alloy; Tool geometry; Nugget zone; Microstructure.

---

[1] Corresponding author: Prof. Mohammad Jahazi, E-mail: mohammad.jahazi@etsmtl.ca, Phone: 514 396-8974

Fax: 514 396-8530

Authors' accepted manuscript of the article published in:
Materials and Design, vol. 58 (2014)
http://dx.doi.org/10.1016/j.matdes.2014.02.005

1. Introduction

Lap joints are widely used in the assembly of parts and products in the transportation industry. Common examples include ship decks, railway tankers and goods wagons, and stringer to skin in aircraft fuselages. For these applications, panels are often straightened with stringers and profiles, which are mechanically or fusion welded joined in a typical lap joint configuration [1, 2]. Friction stir welding (FSW) is an alternative joining process, which has several benefits when compared with mechanical or fusion welding, mainly with regard to the welding of aluminum alloys. Specifically, FSW is a solid-state process where the maximum process temperature does not reach the melting point of the welded materials. Thus, difficulties related to the sensitivity to solidification cracking and the formation of gas porosity, which are very common in fusion welding processes; do not occur in FSW [3, 4]. On the other hand, as it does not require the use of rivets, as in mechanical joining, it results in lower weight for the component and shorter manufacturing times [4].

The process, patented in 1991 by The Welding Institute (TWI), is based on the use of a specially designed rotating tool, characterized by a shoulder and a shaped pin at its end, which is inserted into the adjoining edges of the materials to be joined. The heat flux generated by the combined frictional forces of the rotating shoulder pin and the imposed forge force, plasticize the material beneath the shoulder and moves it around the joint line and the shoulder. In this context, the proper selection of the height and the shape of the pin, (tool geometry), rotating speed and feed rate become critical parameters in optimizing the FSW process [2,3,4]. Among the above parameters, tool geometry can be considered as the most influential process parameter in heat generation and material mixing [5]. The variations in tool design are extensive and combinations of shoulder diameter, shoulder profile, pin length, pin diameter and profile, are all important parameters in determining other welding parameters such as rotational and tool advance speeds as well as the quality of the finished weld. Another important parameter in the determination of the suitability of a tool for a particular application is the tool material itself. Welding is carried out around 70–90% of the base material melting point so it is important that the tool material possess sufficient strength at these temperatures to avoid intense wear or fracture during the FSW process [5].

Because of the important role played by tool geometry in process optimization of FSW, a large number of studies have been reported in the literature on the effect of tool geometry on microstructure evolution and mechanical properties [6-14]. Of particular interest, is the work of Fuji et al. [7] on the effect of tool shape on mechanical and microstructural properties of friction stir welded 1050-H24, 6061-T6, and 5083-O aluminum plates. Although, these studies cover many aluminum alloy series and temper conditions; however, they are mostly limited to butt weld configurations and little has been reported on lap weld configurations and even less for variable thickness and dissimilar temper conditions, which are encountered in industry.

A characteristic feature of friction stir welds in lap mode configuration is the formation of a geometrical defect, called 'hook', originating at the interface of the two welded sheets. During welding, hook(s) could form because of the upward bending of the sheet interface due to the penetration of the tool into the bottom sheet and the concomitant upward movement of the material from the lower sheet to the upper one [15]. Ideally, the oxide film present at the surface of the material should be broken into small and dispersed particles, by the stirring movement of the tool. However, depending on processing conditions, this may not occur and a nearly continuous film of oxides may remain in the intermediate region between the upper and lower sheets. The presence of this defect will prevent the metallurgical bonding and reduce the mechanical properties of the joint. It is clear that, the tool shape significantly affects the hook geometry, which in turn impacts the failure mode and therefore the failure load of friction stir lap welds. Hence, in order to optimize the FSW process of lap welds, it is necessary to develop a better understanding of the formation of the hook defect and the impact of tool geometry on its generation and elimination [16-18].

In the present paper, some of the results related to the influence of tool geometry and rotational speed on defect generation in lap welded AA5456 sheets with different thicknesses and temper conditions are presented. The evolution of the microstructure and mechanical properties as a function of process parameters is studied and the optimum processing conditions are identified. The fracture surface of the failed joints are analyzed by electron microscopy and the microstructural constituents responsible for the degradation of mechanical properties are identified.

2. Experimental procedures

The investigated material was AA 5456 alloy. The material was received in the form of 1200mm long and 500mm wide plates. One of them was 5mm thick and in T321 temper condition (cold worked) and the other one 2.5mm thick in O condition (annealed). The chemical composition and mechanical properties of the material for the two conditions are indicated in Tables 1 and 2 respectively. Specimens 250×250 mm^2 in dimensions were machined from the as-received sheets with their end surfaces machined along the specimen length. The test pieces were first ground using steel brush and sandpaper to remove the oxide films, and then cleaned with acetone to remove any organic residues such as oil. To carry out FSW process, the coupons were fixed on a support plate, which had been fixed on the backing plate of the FSW machine.

The specimens were mounted in lap mode in the configuration shown in Fig.1. All the welds were produced in such a way that the advancing side of the probe was always located near the top sheet edge (ANE). The thinner plate was placed below with an overlap width of approximately 50mm.

In this study, four different friction stir welding tools were designed and manufactured. A schematic of their geometry and their dimensions are shown in Fig.2. Tool geometries similar to T1, T2, and T4 have already been used in the literature [5, 6, 9]; however, in the present research all the tools have threads on their outer surface, which is a new feature. To the knowledge of the authors, the geometry used for the T3 tool is new and has not been previously reported. The shoulder diameter for all four tools was 20mm and the pin length 7 mm corresponding to the intended lap welding depth. The shoulder underside surface was flat and the tilting angle of the probe tool was 3° for all the experiments. Both the shoulder and probe were made of H13 steel to insure pin dimensional stability during the FSW process. The welding direction was perpendicular to the rolling direction of the work piece and all the lap joints were welded using a travel speed of 30 mm/min and rotational speeds of 600 and 800 rpm.

After welding, three tensile shear specimens were wire cut perpendicular to welding direction according to AWS D17.3M:200X standard [19]. This provided samples with a specimen width of 25.4 mm and an overall joint length of approximately 250 mm. To balance the offset axes of the lap specimens and minimize bending effects, two packing pieces with the corresponding thicknesses (5 mm & 2.5mm) were used during the tensile shear testing. The transverse tension tests were performed in a 500 KN capacity servo hydraulic tensile testing machine equipped with side entry hydraulic grips at a speed of 2 mm. min^{-1}. For each tensile shear test specimen, the failure load and fracture locations were recorded. Macrostructural investigation and microstructural studies were carried out using optical microscope and SEM (Scanning electron microscope) equipped with an energy-dispersive X-ray analysis (EDX) system. For microstructural studies, samples were cut and polished according to standard metallographic techniques. They were all etched using a solution composed of 35 ml HNO3, and 65 ml H2O under warm conditions.

3. Results and discussion

3.1. Effect of pin geometry on the macrostructure of FSW joint

Pin profile plays a crucial role in material flow and in turn regulates the welding speed of the FSW process. Pin geometry influences the nugget macrostructure greatly. Fig. 3 and Fig. 4 show the cross section macrographs of the joint welded with the four different tools used in the investigation for the two rotational speeds of 600 and 800 rpm, respectively. As indicated, no voids, cracks or other common weld defects were seen in the welded joints except for the T4 tool at 800 rpm, as shown in Fig. 4d.

The cross section of the weld joint can be divided into four regions: the base metal, the heat-affected zone (HAZ), the thermo-mechanically-affected zone (TMAZ) and the weld nugget (WN). One of the most common defects observed in friction stir welded lap joints is hooking. This defect is observed in TMAZ and WN. Its occurrence in the TMAZ of the advancing side has been associated with the upward movement of the joint interface towards the top sheet (i.e. upward material flow) [20]. While its occurrence in the nugget zone has been associated with changes in material flow direction, from downward to upward, depending on tool geometry and welding conditions (hot or cold) [21]. The differences in the hook defect characteristics (Shape and height) can be attributed to the amount of material flow produced in the stir zone by the rotating tool [6, 9, 12]. Due to the presence of threads on the pin surface, which enhances plastic flow in the thickness direction resulting in better stirring, and also the tool geometry used in the present study, material flow occurred by downward movement from the upper sheet to the lower one and immediately pushed upward towards the upper sheet thereby affecting the hooking height. Similar findings have been also reported by [16].

Hooking defects with different sizes were found in welded joints and are indicated in Figs. 3 and 4. Their average heights as a function of tool type and processing conditions were measured and are reported in Fig.5. Also in this figure, the lower plate effective thickness, ET, (defined as the distance between the mid height point of the hook and the position of interface between the two sheets) is reported. This parameter is very important as it affects the static strength of the weld joint. Indeed, a higher value for ET indicates that a larger size hook defect and thus, a more negative impact on mechanical properties (see Table 3).

Examination of the data in Fig.5 shows that, the lower plate effective thickness is not constant and changes significantly with the tool geometry confirming that pin geometry affects material movement and the extent of the imposed plastic deformation. Therefore, the hooking height and the effective plate thickness will change which ultimately would affect joint strength. The results also show that the lowest hooking height and plate effective thickness are obtained with the T3 tool. The origin of the hooking defect being related to material flow which is dependent on welding conditions and tool geometry, it is reasonable to assume that with the new tool geometry better material mixing has occurred resulting in less unidirectional material movement from the joint interface towards the upper sheet and hence lower hook height. Fig. 6 shows the variation of hooking heights for different tool geometries, for the two investigated rotational speeds. In the welds produced by the three other tools, the hooking defects are of larger size (i.e. higher hook height). In addition to its height, the slope of a hook could also be considered (Fig.7) as an evaluation criterion for the quality of a lap weld. In fact, during tensile testing, the angle between the hook axis and the applied tensile load (hook slope) will have a determining influence on the mechanical properties of the joint.

In addition to hooking defects, film like flaws were detected and are shown in Figs. 3 and 4. Other authors have also observed such defects and related their origin to the thin oxide film present on the faying surfaces that are not affected by the stirring tool [22]. Film like flaws in the central nugget of the FSW (Figs. 3 and 4) are relatively small, have irregular morphology, erratic length, and can be aligned with the flow contours within the nugget. In the present investigation, it was found that these defects were in the central region of the nugget when T1, T2 and T4 tools were used. By contrast, they were only observed on the advancing side of the weld nugget when T3 tool was used. The breakdown of the continuous oxide film at the faying surface because of the stirring movement of the pin, produce also fine oxide particles which are then dispersed into the weld nugget. Therefore, because pin profile influences plastic deformation and material mixing during the process, consequently, the volume and distribution of these particles would vary as a function of tool geometry. It is anticipated that, the T3 tool because of its design, would improve material mixing and enhance the upward movement of material from the lower sheet to upper one compared to the other 3 tools. Fig. 8 shows two illustrative examples of the influence of pin shape on the form and distribution of film like flaws and hooking defect for two experimental conditions (T4 tool, 600 rpm, T1 tool, 800 rpm).

The weld interface region was also examined by SEM and the presence of defects correlated with material flow conditions. Specifically, Fig. 9 shows the macro cross sections of friction stir weld zone (Fig.9a) and the SEM micrograph (Fig.9b) from the retreating side of the weld in the identified region in Fig8a. The presence of interface voids containing oxide films is clearly revealed. These oxides may come from the original plates, even though all joint surfaces were cleaned before FSW, and/or produced by micro oxidation of the surfaces along the interface during welding. The presence of oxide particles at the interface, deteriorates joint quality and produces a region of weakness that can affect the mechanical properties of weld joint and decreases the joint strength during tension test [14]

3.2. Effect of the pin geometry on mechanical properties

The tensile shear force of joints made with the four friction stir tools and for the two rotational speeds are compared in Fig. 10. For each condition, at least three specimens were tested, and the average results are presented. The results indicate that, the joints fabricated by stepped conical thread pin (T3 tool) exhibited superior tensile properties compared to the other ones. Irrespective of tool rotational speed, specifically for the samples welded by T3 tool, the value of the tensile shear force reached 21250 N (failure load), which is equivalent to that of the lower base metal. As a result, in this case, the fracture occurred from the base metal in the lower plate. The joints obtained by using T1, T2, and T4 tools, exhibited inferior tensile properties and cracking occurred in the retreating side of the weld joint. This can be related to the position and intensity of the hooking defect in the weld. The obtained results, in all the welded joints, suggest that hooking defects in the advancing side were stopped after they reached the nugget zone. By contrast, those in the retreating side, extended to the center of the nugget zone with various intensity for all the welded joints. On the basis of the obtained results, the hook geometry could be considered as a criterion to describe the failure mechanism in friction stir lap welded joints.

The hook defect, which exists between overlapped sheets, is a weak metallurgical bond and can act as a crack as it has already proposed by other authors [16-18]. Initially, at low levels of external loads, the crack can propagate along the hook in the two sides of the weld. However, in the advancing side, it does not lead to failure because, it is limited by the boundary between the TMAZ and the nugget zone. Conversely, in the retreating side (Figs.3 and 4), hooking defect goes towards the center of the nugget zone at the bottom of the weld region and propagates in the hook direction [15].

Based on the above observations, it can be stated that the difference in mechanical resistance of FSW lap joints is due to changes in material flow occurring in the transverse directions of the joints and especially on their retreating sides during the welding process. The best mechanical performances were obtained when using T3 tool. This could be due to different design elements consisting of the combination of the conical and cylindrical shape geometry, threaded pin, and the existence the step size proportional to the interface height between the two sheets. The proposed tool geometry appears to have resulted in an optimized upper movement of the material and its mixing in the nugget zone, and therefore to the observed higher mechanical strength for the weld joints produced by the T3 tool. Tensile testing of the joints welded by T3 tool showed that fracture occurred on the lower base metal sheet with 2.5mm thickness (Fig.11.a). In the case of the joints produced by the T2 tool, the results indicate that fracture occurred from hooking in the retreating side. Crack propagation has most probably also occurred in the advancing side; however fracture was only observed on the hooks present in the retreating side [15].

3.3 Influence of tool geometry on particles fragmentation

The fracture surfaces of samples welded by T3 tool are shown in Figs.12 (a and b). As indicated in Fig. 12a, a large number of dimples present on fracture surface, indicating a ductile behavior. Most of the dimples have a homogeneous distribution, are fine and have approximately an equiaxed pattern. This finding is in agreement and confirms the superior mechanical properties obtained under these conditions (600rpm, T3 tool). By contrast, as shown in Fig.13, under the same FSW conditions, the fracture surface of the specimens produced using T2 and T4 tools contains heterogeneous dimple sizes and shapes with fragmented particles of different sizes.

SEM examination of the distribution of intermetallic particles (e.g. Fig 12b) in the microstructure of the welds obtained by the four investigated tools revealed that the fragmented brittle intermetallic particles are more dispersed and are finer when T3 tool is used. This is probably due to more stirring and plastic deformation caused by this tool compared to the three others. These findings are in agreement with those reported by Zho et al. [10] and Boz and court [11]. As indicated in Fig.13, the closer proximity and larger size of these particles may be at the source of crack initiation during the tensile shear test. Exact quantification of the influence of tool geometry on material plasticity is very complex [13] and out of the context of this paper; however, our results clearly indicate that among the four investigated geometries, improved material flow and particle fragmentation and dispersion, were obtained with the T3 tool.

Chemical analysis of the particles by EDX, revealed that they are $(FeMn)_3SiAl_{12}$ intermetallics (point A in Fig. 13a shown in Fig. 14). The presence of such intermetallics in 5xxx series aluminum alloys has already been reported by other authors [23]. They are amorphous structure but transform to crystalline one after long holding times at high temperature [23]. However, FSW is characterized by relatively rapid heating and cooling cycles and low heat input and as such it is not expected that it will be possible to transform the amorphous intermetallic particles during FSW. Therefore, such particles remain without any structural changes and are only fragmented and redistributed during the stirring process.

4. Conclusions

Aluminum alloy 5456plates with different tempers (T321 & O) and thicknesses were joined in lap configuration using friction stir welding process. Four different pins were designed to study the influences of pin geometry on hook defect characteristics, weld nugget shape, structural and mechanical properties of the joints.

(1) Of the four tool pin profiles used in this investigation the highest joint performances were obtained with the stepped conical threaded pin (tool T3) introduced in the present investigation.

(2) The different design elements, consisting of the combination of the conical and cylindrical shape geometry, threaded pin, and a step size proportional to the interface height between the two sheets, are probably responsible for higher contact surface and better plasticity of the material in the case of tool T3.

(3) Of the two tool rotational speeds used in this investigation, the joint fabricated with the rotational speed of 600 rpm, showed better tensile properties irrespective of tool pin profile.

(4) Hook defect height and effective lower plate thickness were used as a quality criterion for the welded joints.

The obtained results clearly indicate the beneficial effects of the stepped conical thread pin on joint integrity and mechanical properties through improved material flow during FSW. Thus a more fundamental understanding of material flow during FSW using the above tool is necessary in order to develop material models needed for simulation of the process for industrial size components. To this end, it will be very interesting to design experiments with the view to document and quantify the influence of each process parameter on material flow, defect generation, and microstructure evolution.

References

[1] Thomas WM, Norris IM, Stains DG, Watts ER. Friction Stir Welding-Process developments and techniques. The SME summit. Oconomowoc, Milwaukee, 2005; 1-21.

[2] Buffa G, Campanile G, Fratini L, Prisco A. Friction stir welding of lap joints: Influence of process parameters on the metallurgical and mechanical properties. Materials Science and Engineering A 2009; 519: 19-26.

[3] Abdollah-Zadeh A, Saeid T, Sazgari B. Microstructural and mechanical properties of friction stir welded aluminum/copper lap joints. Journal of Alloys and Compounds 2008; 460: 535-8.

[4] Leal RM, Loureiro A. Effect of overlapping friction stir welding passes in the quality of welds of aluminium alloys. Materials and Design 2008; 29: 982-91.

[5] Bahemmat P, Rahbari A, Hagh panahi M, Besharati MK. Experimental study on the effect of rotational speed and tool pin profile on AA2024 aluminum friction stir welded butt joints. Proceedings of ECTC ASME early career technical conference 2008; Miami, Florida, USA.

[6] Padmanaban G, Balasubramanian V. Selection of FSW tool pin profile, shoulder diameter and material for joining AZ31B magnesium alloy - An experimental approach. Materials and Design 2009; 30: 2647–56.

[7] Fujii H, Ling Cui L, Masakatsu Maeda M, Kiyoshi Nogi K. Effect of tool shape on mechanical properties and microstructure of friction stir welded aluminum alloys. Materials Science and Engineering A 2006; 419: 25–31.

[8] Scialpi A, Filippis LACD, Cavaliere P, Influence of shoulder geometry on microstructure and mechanical properties of friction stir welded 6082 aluminum alloy. Materials and Design 2007; 28: 1124–1129.

[9] Elangovan K, Balasubramanian V. Influences of pin profile and rotational speed of the tool on the formation of friction stir processing zone in AA2219 aluminium alloy. Materials Science and Engineering A 2007; 459: 7–18.

[10] Zhao YH, Lin SB, Wu L, Qu FX, The influence of pin geometry on bonding and mechanical properties in friction stir weld 2014 Al alloy. Materials Letters 2005; 59: 2948 -52.

[11] Boz M, Kurt A. The influence of stirrer geometry on bonding and mechanical properties in friction stir welding process. Materials and Design 2004; 25: 343-7.

[12] Elangovan K, V. Balasubramanian V. Influences of tool pin profile and tool shoulder diameter on the formation of friction stir processing zone in AA6061 aluminium alloy. Materials and Design 2008; 29: 362-73.

[13] Kumar K, Kailas SV. The role of friction stir welding tool on material flow and weld formation. Materials Science and Engineering A 2008; 485: 367-74.

[14] Ali A, Brown MW, Rodopoulos CA, Gardiner S, J Fail Anal Prev 2006; 6-4: 83-96.

[15] Dubourg L, Merati A, Jahazi M. Process Optimization and Mechanical Properties of Friction Stir Lap Welds of 7075-T6 Stringers on 2024-T3 Skin. Materials and Design 2010; 31-7: 3324-30.

[16] Chionopoulos SK, Sarafoglou CHI, Pantelis DI, Papazoglou VJ. Effect of tool pin and welding parameters on friction stir welded (FSW) marine aluminum alloys. Proceedings of the 3rd International Conference on Manufacturing Engineering (ICMEN) 2008; Chalkidiki, Greece.

[17] Badarinarayan H, Shi Y, Li X, Okamoto K, Effect of tool geometry on hook formation and static strength of friction stir spot welded aluminum 5754-O sheets. International Journal of Machine Tools and Manufacture 2009; 49: 814-23.

[18] Cao X, Jahazi M. Effect of tool rotational speed and probe length on lap joint quality of a friction stir welded magnesium alloy. Materials and Design 2011; 32: 1-11.

[19] AWS D17.3/D17.3M:2010. Specification for Friction Stir Welding of Aluminum Alloys for Aerospace Applications. American Welding Society (AWS) 2009, Miami, Florida, USA.

[20] Bisadi M, Tour M, Tavakoli A, The influence of process parameters on microstructure and mechanical properties of 5083 Al alloy, American Journal of Materials Science, 2011; 1: 93-7.

[21] Arbegast WJ, A flow partitioned deformation zone model for defect formation during FSW, Scripta Materialia, 2008; 58: 372-6.

[22] GMD Cantin SA David, Thomas WM, Curzio EL, Babu SS. Friction Skew-stir welding of lap joints in 5083–0 aluminum, Science and Technology of Welding and Joining. 2005; 10-3: 268-80.
[23] Badarinarayan H, Yang Q, Zhu S, Effect of tool geometry on static strength of friction stir spot-welded aluminum alloy, International Journal of Machine Tools and Manufacture 2009; 49: 142-8.

Figures captions

Fig. 1. Schematic of lap mode.

Fig. 2. Geometry and technical details of the investigated tools.

Fig.3. Macro cross sections of friction stir weld zone under rotational speed 600 rpm Welded by (a) T1. (b) T2. (c) T3. (d) T4 (AS: advanced side and RS: retreated side, H.H: Hooking height, θ: Hooking Slope).

Fig.4. Transverse sections of friction stir weld zone under rotational speed 800 rpm Welded by (a) T1. (b) T2. (c) T3. (d) T4 (AS: advanced side and RS: retreated side, H.H: Hooking height, θ: Hooking Slope).

Fig. 5. Hooking height (H.H) and lower plate effective thickness (ET) per mm for different tools and rotational speeds.

Fig. 6. Hooking heights for 4 different tools.

Fig. 7. Hooking slopes for 4 different tools.

Fig.8. Optical micrographs showing a path of interface on retreating side of weld nugget (showing film like Flaws), a: by using T4 tool and under 600 rpm rotational speed, b: by using T1 tool and under 800 rpm rotational speed.

Fig. 9. a) Macro cross sections of friction stir weld zone under rotational speed 600 rpm Welded by T3 tool and b) back scattered SEM images showing interface voids on retreating side.

Fig. 10. Results of tensile tests by using 4 different tools and under (a). 600 rpm and (b). 800 rpm rotational speed.

Fig. 11. Fracture from different regions on joints.

Fig. 12. Fracture morphology of fracture plane using T3 tool and under 600rpm rotational speed.

Fig. 13. Fracture morphology of fracture plane using (a). T2 tool and (b). T4 tool, under 600rpm rotational speed.

Fig. 14. The EDX spectrum analysis of ‘A’ region in Fig. 13a.

Tables captions

Table 1. Chemical compositions of aluminum alloys

Table 2. Mechanical properties of aluminum alloys

Table 3. Hooking slopes for different tools and rotational speeds.

Table 1. Chemical compositions of aluminum alloys

Type	Chemical composition in Wt.%					
	Al	Mg	Mn	Cu	Fe	Si
5456- T321	Bal	4.81	0.63	0.01	0.20	0.08
5456- O	Bal	4.79	0.50	0.02	0.18	0.12

Table 2. Mechanical properties of aluminum alloys

Type	Failure Load (N)	Elongation (%)	Hardness at 200 gr load (HV)
Base Plate 2.5mm	21250	35	89
Base Plate 5mm	50500	16	140

Table 3. Hooking slopes for different tools and rotational speeds.

Rotational speed (rpm)	Tools (Degree)			
	T1	T2	T3	T4
600 rpm	46.37	31.93	8.21	49.14
800 rpm	47.81	38.34	10.68	42.42

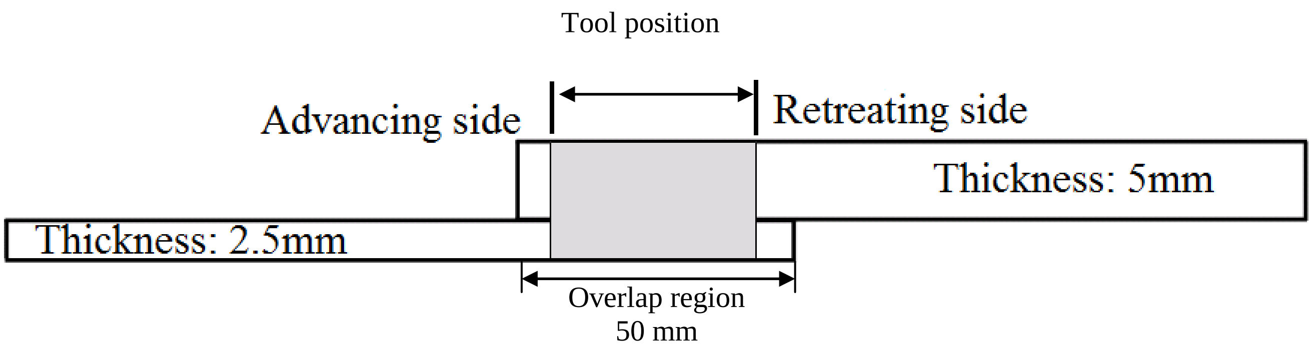

Fig. 1. Schematic of lap mode.

Tools	Description of the pin	Big diameter of the pin (mm)	Small diameter of the pin (mm)	Pitch of the pin (mm)
T1	Conical screw thread pin	7	5	0.8
T2	Cylindrical–conical thread pin	7	5	0.8
T3	Stepped conical thread pin	7.5	4	0.8
T4	Neutral Flared-Triflute pin	7	5	0.8

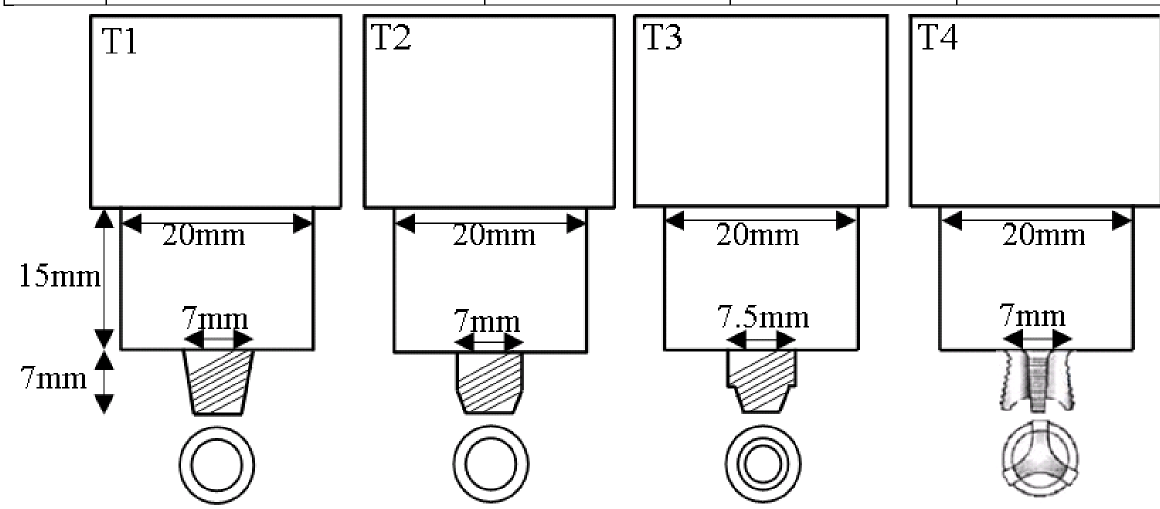

Fig. 2. Geometry and technical details of the investigated tools.

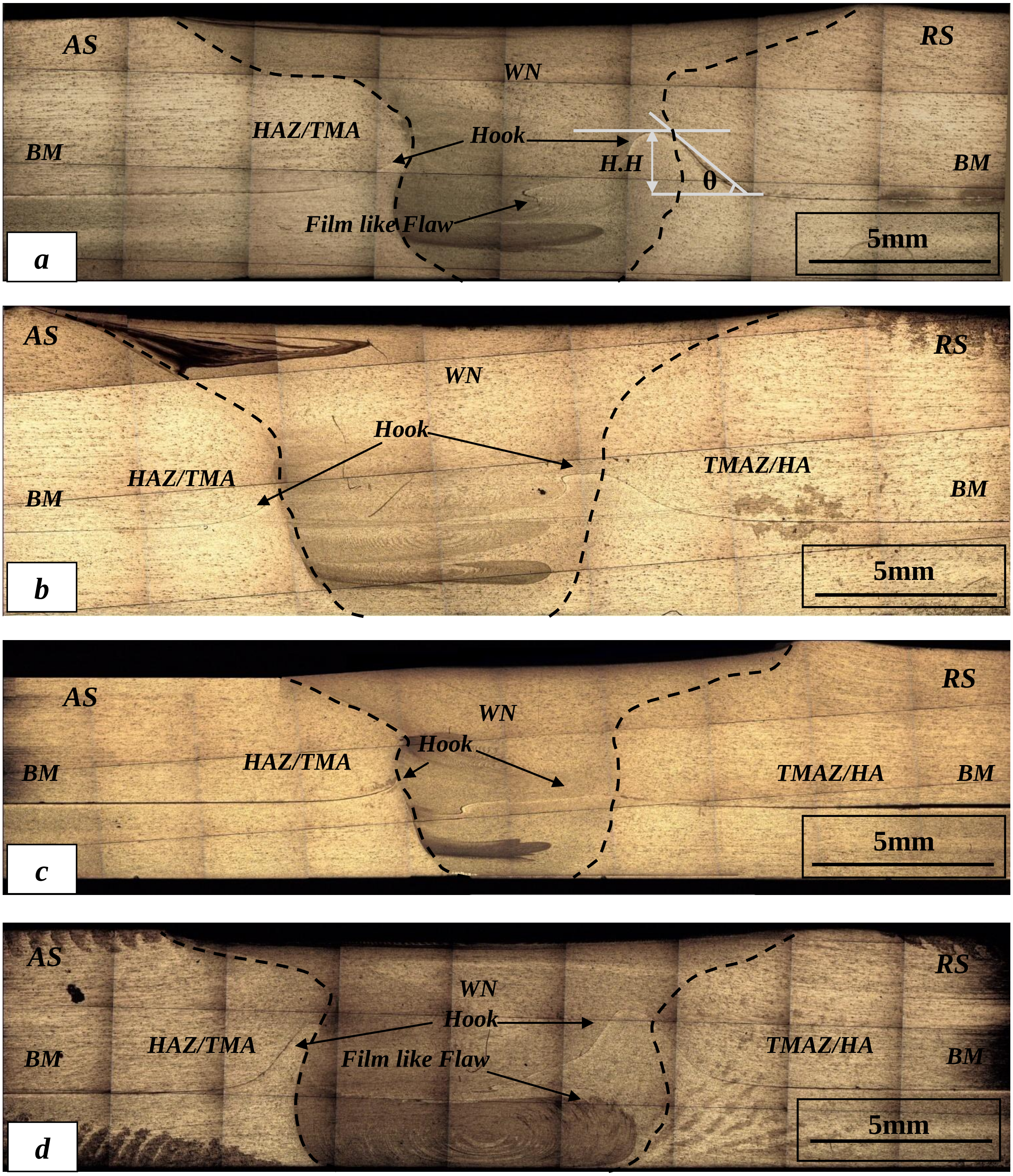

Fig.3. Macro cross sections of friction stir weld zone under rotational speed 600 rpm Welded by (a) T1. (b) T2. (c) T3. (d) T4 (AS: advanced side and RS: retreated side, H.H: Hooking height, θ: Hooking Slope).

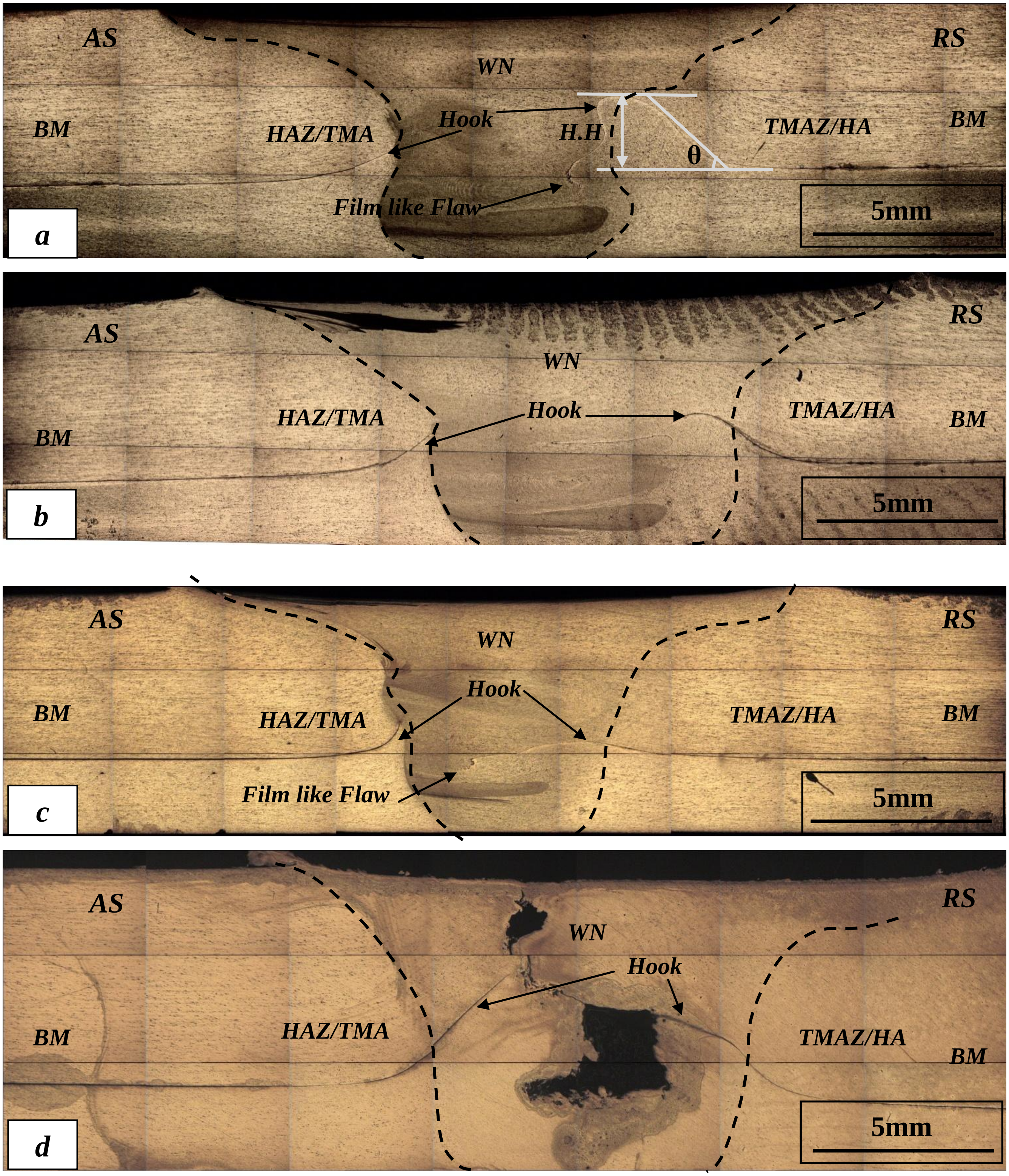

Fig.4. Transverse sections of friction stir weld zone under rotational speed 800 rpm Welded by (a) T1. (b) T2. (c) T3. (d) T4 (AS: advanced side and RS: retreated side, H.H: Hooking height, θ: Hooking Slope).

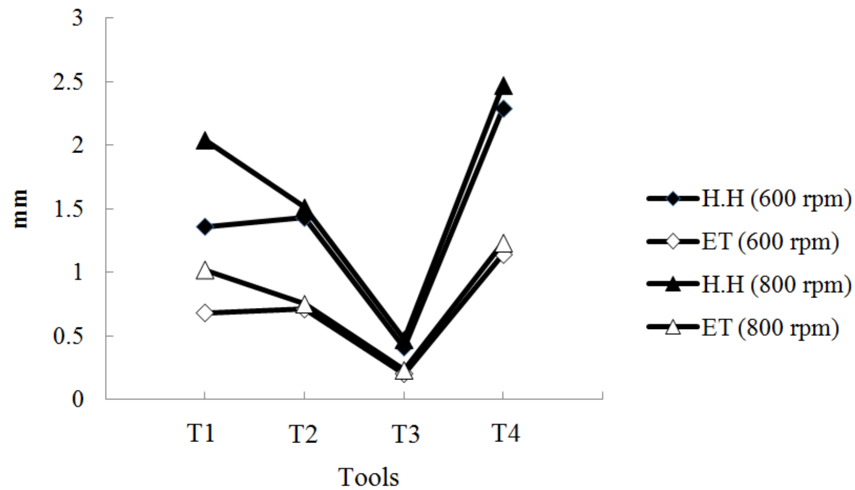

Fig.5. Hooking height (H.H) and lower plate effective thickness (ET) per mm for different tools and rotational speeds.

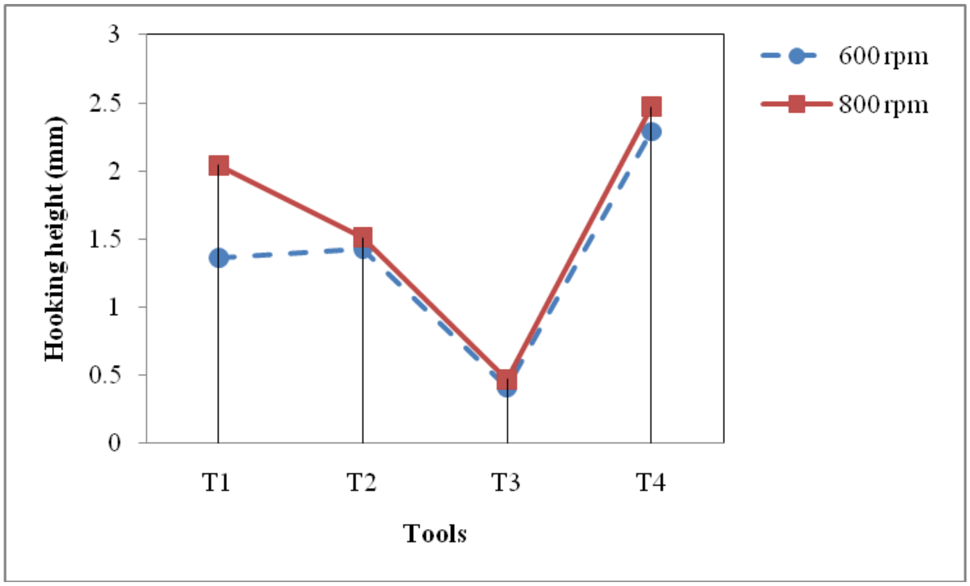

Fig. 6. Hooking heights for 4 different tools.

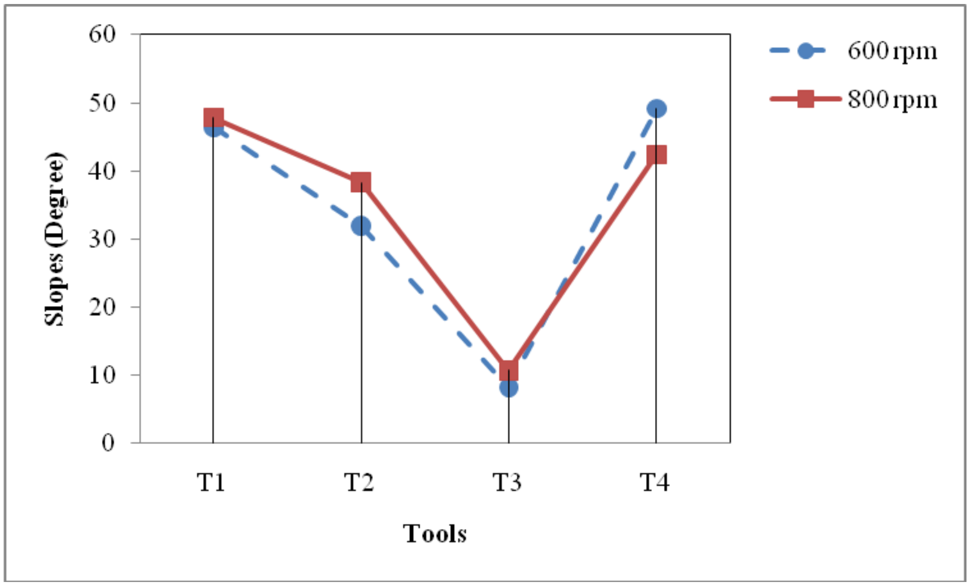

Fig. 7. Hooking slopes for 4 different tools.

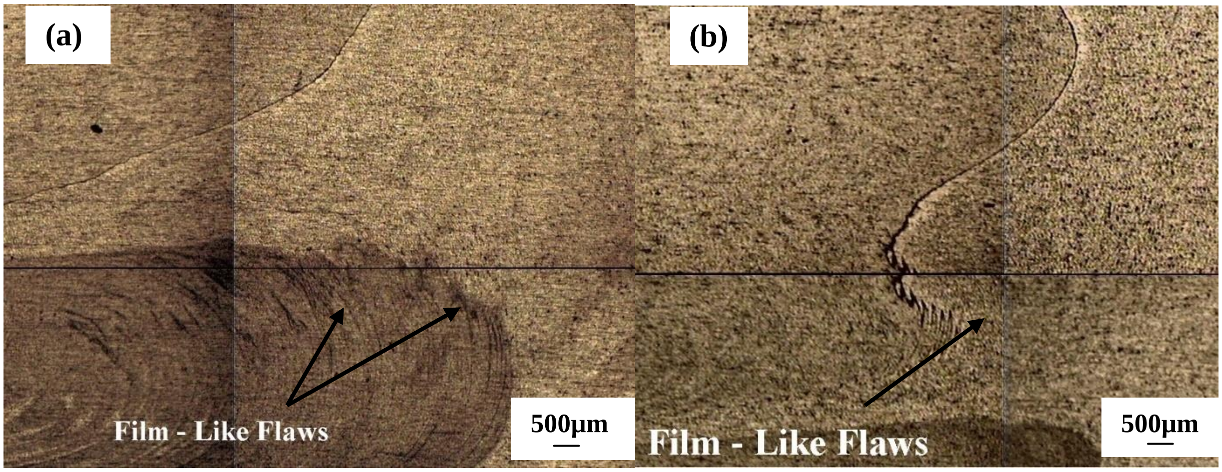

Fig.8. Optical micrographs showing a path of interface on retreating side of weld nugget (showing film like Flaws), a: by using T4 tool and under 600 rpm rotational speed, b: by using T1 tool and under 800 rpm rotational speed.

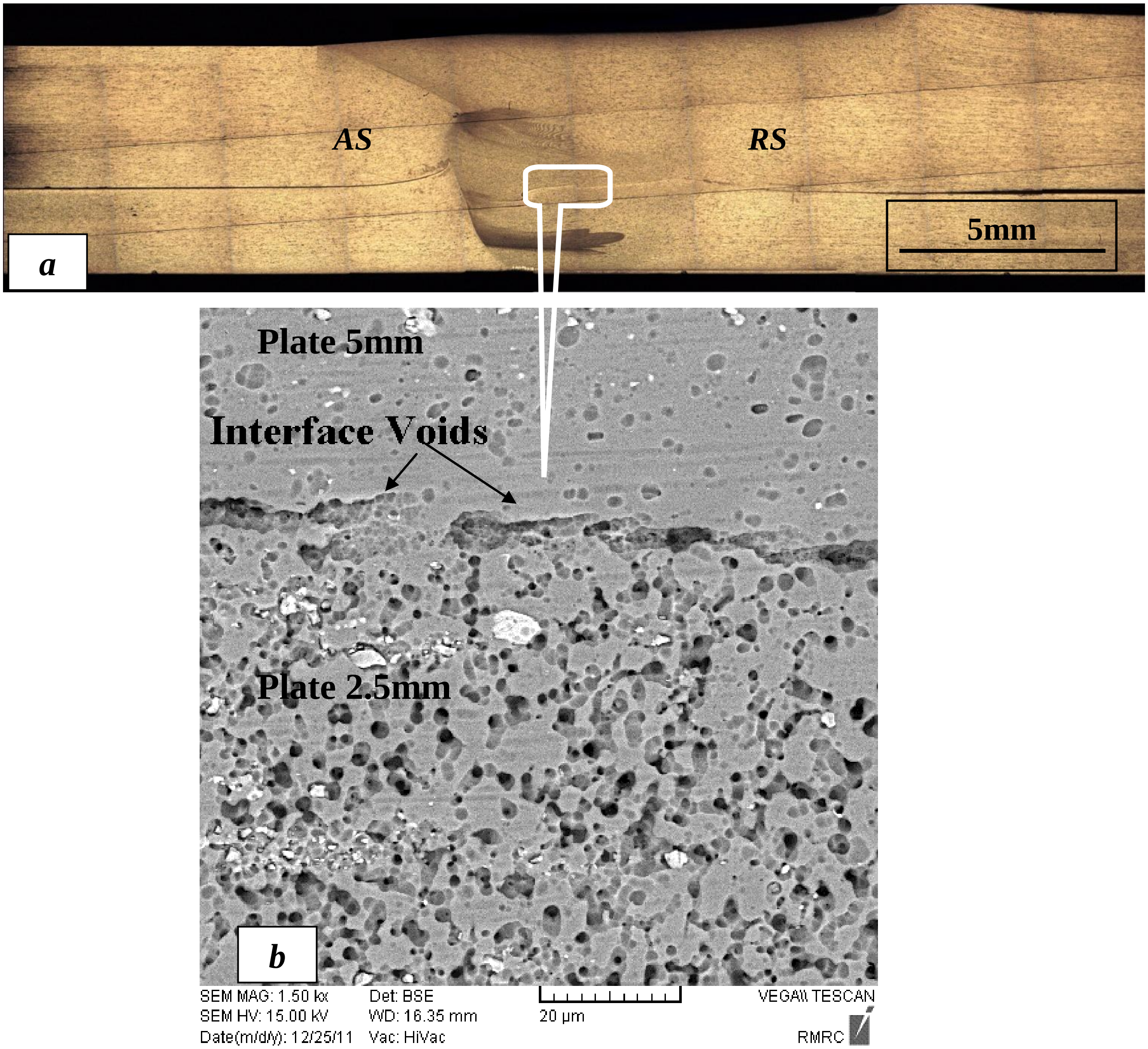

Fig. 9. a) Macro cross sections of friction stir weld zone under rotational speed 600 rpm Welded by T3 tool and b) back scattered SEM images showing interface voids on retreating side.

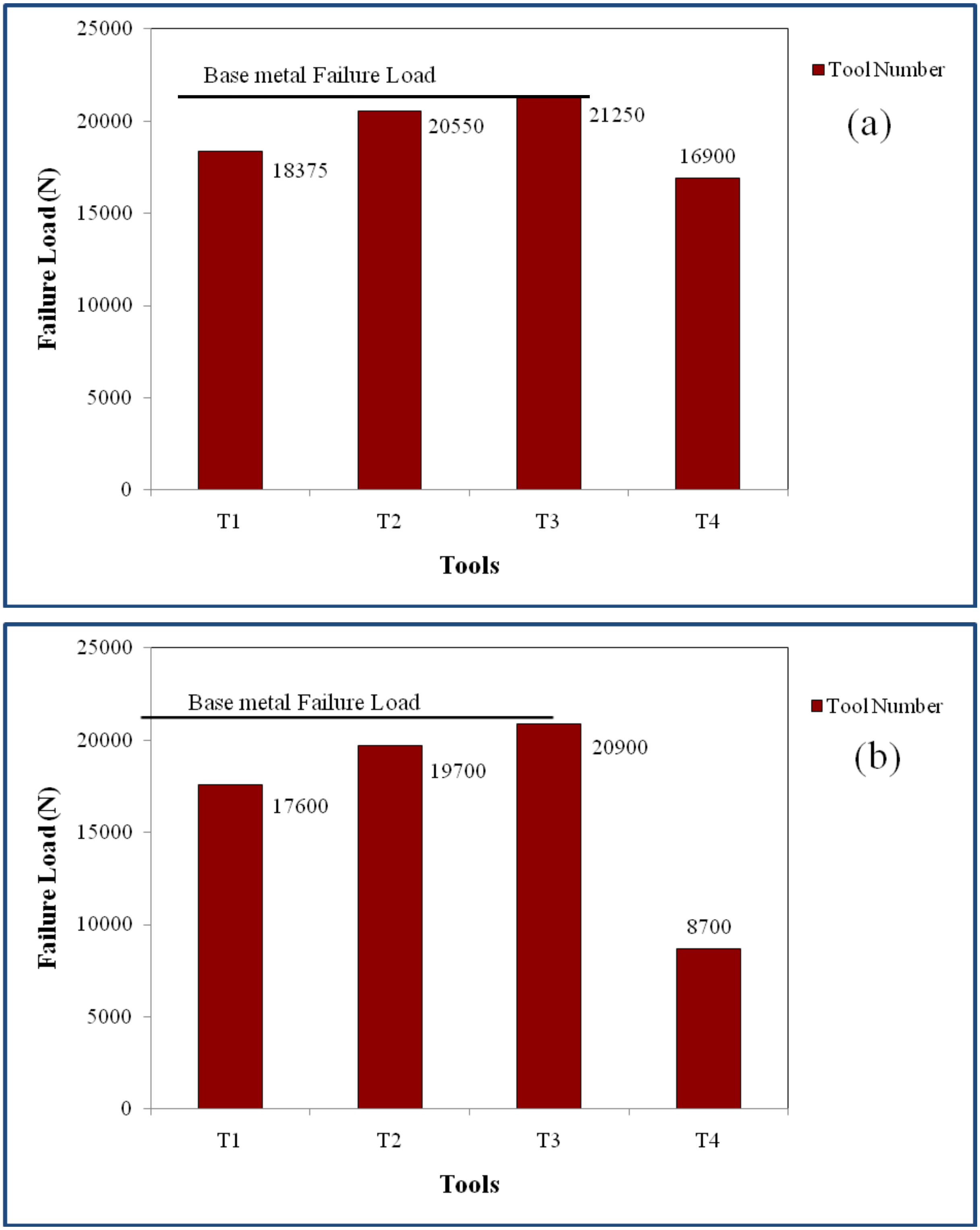

Fig. 10. Results of tensile tests by using 4 different tools and under (a). 600 rpm and (b). 800 rpm rotational speed.

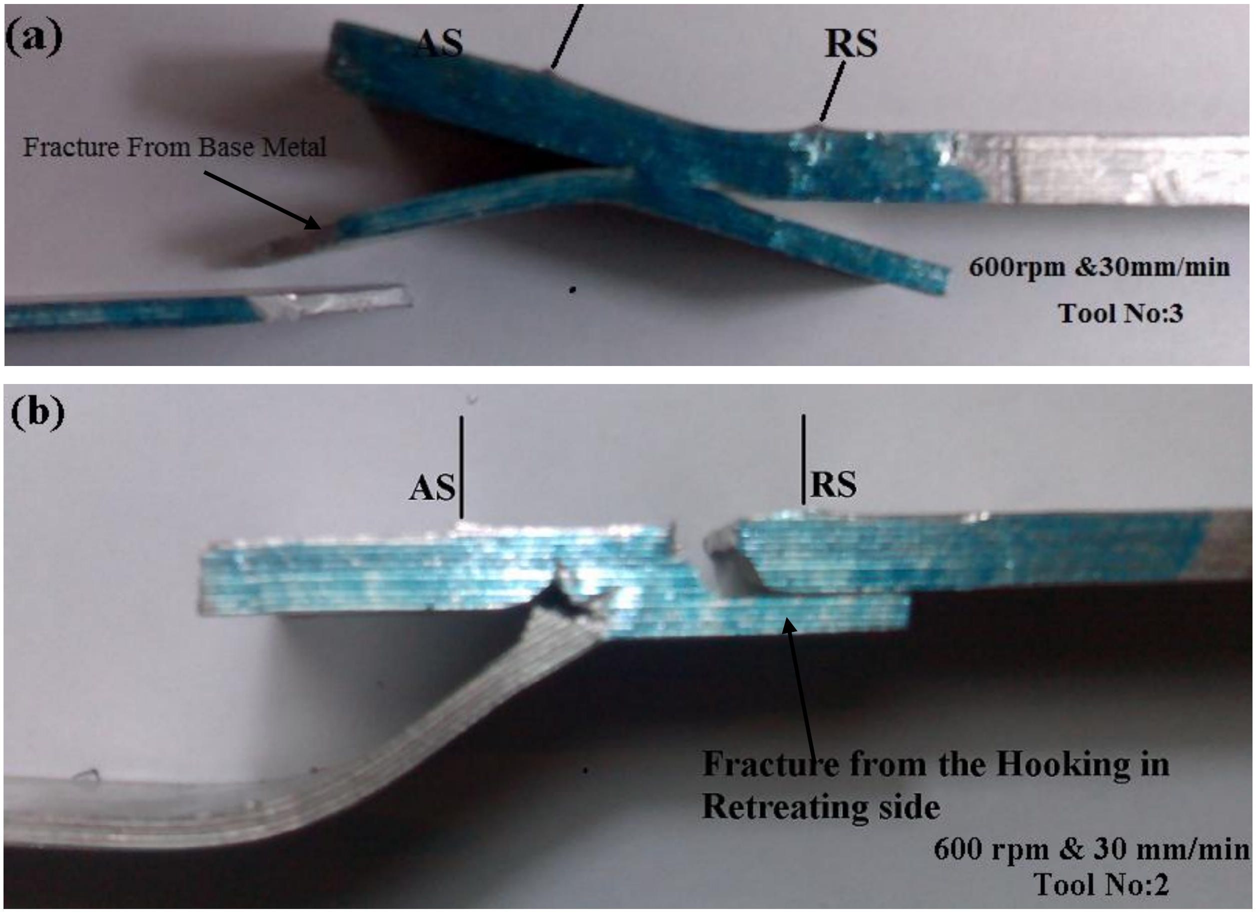

Fig. 11. Fracture from different regions on joints.

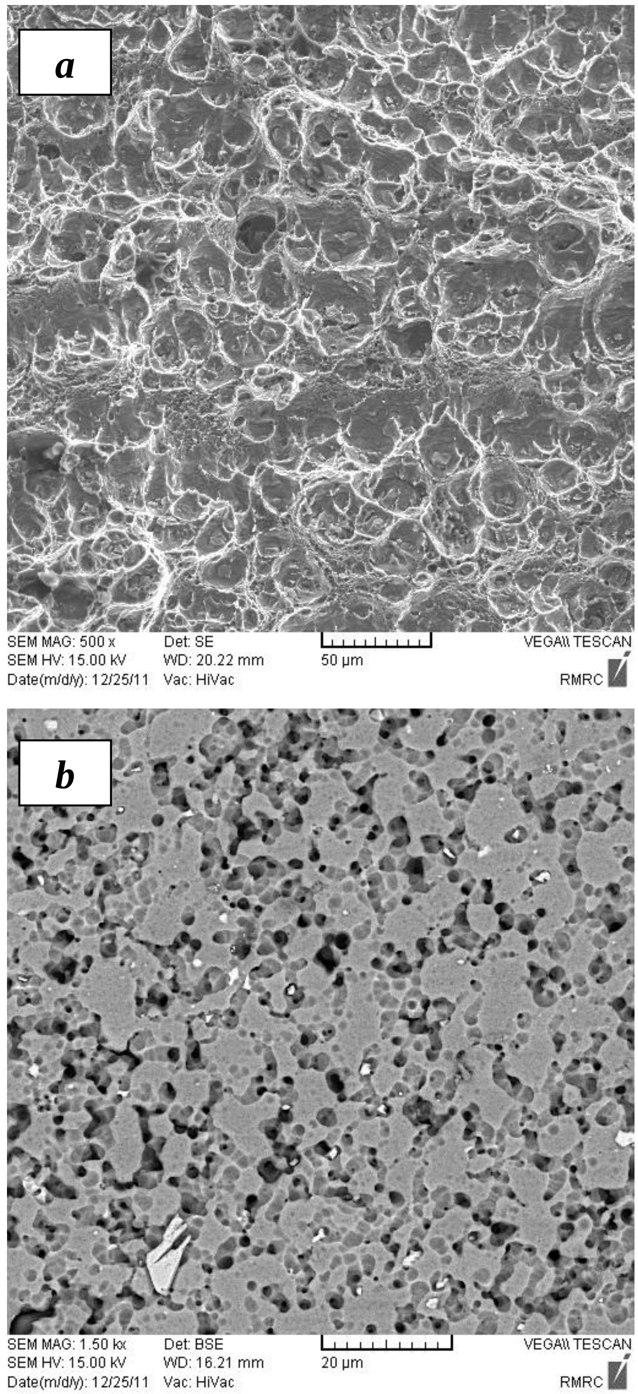

Fig. 12. Fracture morphology of fracture plane using T3 tool and under 600rpm rotational speed.

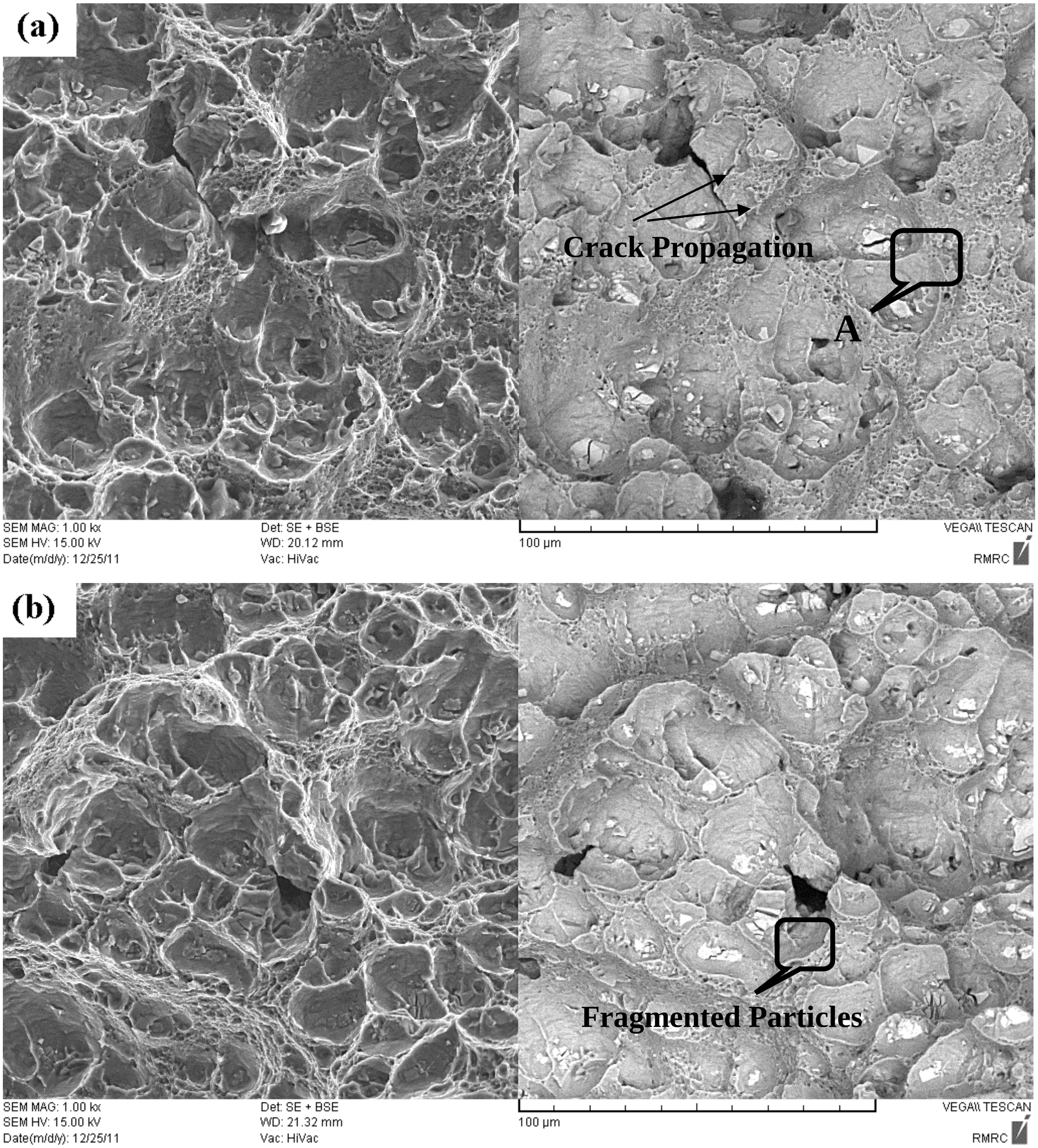

Fig. 13. Fracture morphology of fracture plane using (a). T2 tool and (b). T4 tool, under 600rpm rotational speed.

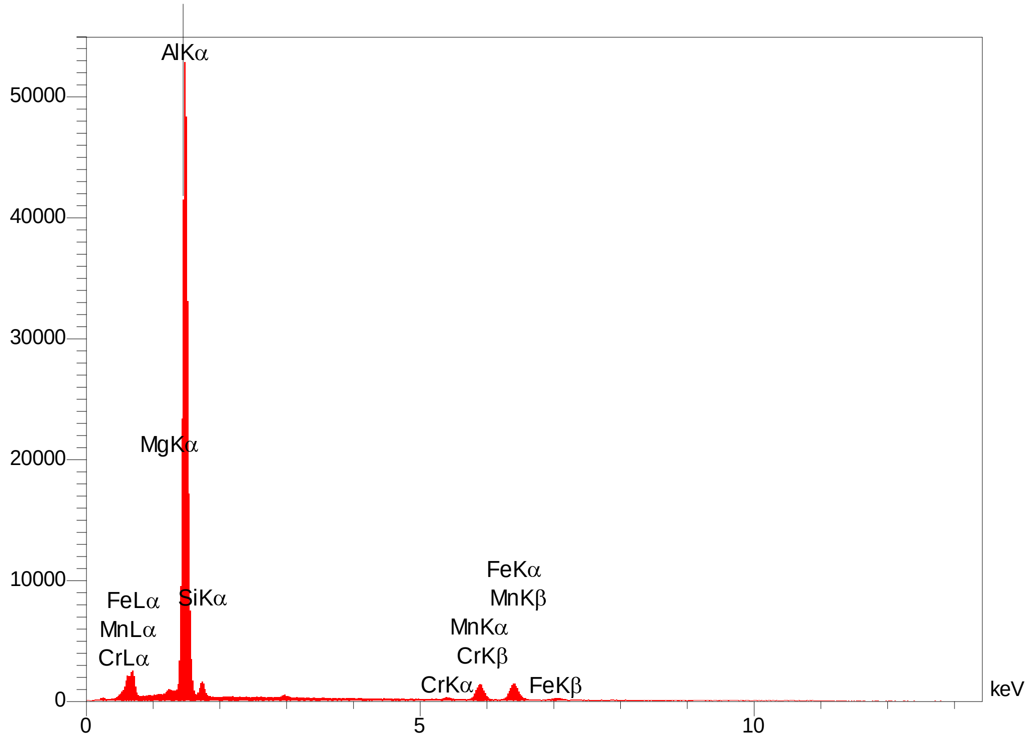

Fig. 14. The EDX spectrum analysis of 'A' region in Fig. 13a.